Copper plasmonics with excitons

David Ziemkiewicz* and Sylwia Zielińska-Raczyńska
Institute of Mathematics and Physics, Technical University of Bydgoszcz, Al. Prof. S. Kaliskiego 7, 85-789 Bydgoszcz, Poland

(Received 17 August 2022; revised 1 October 2022; accepted 31 October 2022; published 7 November 2022)

We investigate the propagation of surface plasmons in a thin layer of copper surrounded by copper oxide Cu_2O. It is shown that particularly strong excitons in Cu_2O can have a considerable impact on plasmon propagation, providing many opportunities for plasmon-exciton and plasmon-plasmon interactions. It is demonstrated that by the use of a sufficiently thin metal layer, one can excite the so-called long range plasmons, which can overcome the inherently high ohmic losses of Cu as compared to the usual plasmonic metals such as silver. Analytical results are confirmed by numerical calculations.

DOI: 10.1103/PhysRevB.106.205404

I. INTRODUCTION

The surface plasmon-polaritons (SPPs) are bound, nonradiative electromagnetic excitations associated with charge density waves propagating along the metal/dielectric interface. It is well known that surface plasmons can be used to confine the field of the electromagnetic wave into subwavelength areas, greatly increasing field intensity and as a result the intensity of the electromagnetic field is enhanced. Plasmonic devices offer many significant advantages in solid-state device applications; an electromagnetic wave bound to a metallic surface can be not only focused, but also easily guided or slowed down. All these properties are very useful for providing a favorable environment for the light-exciton interaction. The development of applications where both energy propagation and field confinement are desired requires a detailed analysis of the trade-off between the two. This interchange is a direct consequence of a field confinement and plasmon propagation being reciprocal to each other, i.e., propagating SPPs assume a localized character in the frequency region of the surface plasmon while as confinement gets stronger, the electric field penetrates deeper into the metal (surface), leading to increased energy losses. While noble metals are the most popular among plasmonic materials, copper-based plasmonic devices are a recent, dynamically expanding area of research, with promising applications in nanoantennas [1], photovoltaics [2,3], and waveguides [4].

A nontrivial aspect of design copper-based devices is the surface protection from oxidation. Various protective layers were proposed, including graphene [5]. Without the oxide layer, Cu nanostructures exhibit a narrow plasmonic resonance comparable to the one found in silver and gold nanostructures [6]. On the other hand, a controlled layer of oxide with a specific thickness might enhance the plasmonic resonance instead of perturbing it [7,8]. The ongoing research towards the reduction of ohmic losses in copper nanostructures leads to geometries that can match the performance of the usual plasmonic materials such as gold and silver [9].

An exciton in a semiconductor is a bound state of a conduction band electron and a valence band hole, which are attracted to each other by the Coulomb interaction; they form an electrically neutral quasiparticle, transferring the energy without transporting the net electric charge. The ability to couple plasmons with excitons, creating so-called plexcitons [10,11], leads to a variety of plasmonic devices that can be tuned on demand [12–14]. Exciton-plasmon coupling was demonstrated in the case of Wannier excitons in semiconductors [15], but the use of copper oxide, in particular Cu-Cu_2O structures is a novel idea. Excitonic states in Cu_2O are a solid-state analog of hydrogen atoms and states with principal quantum number up to $n = 25$ for dipole-allowed P-type envelope wave functions, called Rydberg excitons (REs), were observed [16]. Rydberg excitons are becoming one of the most versatile, scalable, and tunable platforms for quantum computing technologies. The field is developing very rapidly, with first theoretical studies [17,18] and experiments [19,20] exploring the nonlinear properties of RE in low-dimensional systems being performed right now. The fabrication techniques are just entering the stage where consistent synthesis of high-quality Cu_2O nanostructures becomes possible [21,22]. Furthermore, from a more general point of view, Rydberg excitons are one-of-a-kind structures that may offer new insight into fundamental physics; their huge dimension make them an ideal candidate for performing experiments with spatially engineered light fields and micrometer-sized plasmonic systems. The prominent idea of this paper is to take advantage of their unusual properties coupling these structures with plasmons

The paper is organized as follows. In the next section the basic properties of Rydberg excitons important to the propagation of plasmons are discussed and some general limitations of the system are outlined. Next, the dispersive properties of plasmons excited on a thin metal layer are investigated focusing on the specific case of copper surrounded by copper oxide. Section IV contains calculation results. The last section presents the summary of our results. Finally, the details of the employed finite-difference time-domain (FDTD) numerical method are given in Appendix.

*david.ziemkiewicz@utp.edu.pl

II. EXCITONS AND RYDBERG BLOCKADE

An exciton is an excited electronic state of the crystal is an electron-hole pair, which is weakly bound and can extend over many thousands of lattice unit cells, thus its interaction is screened by static permittivity of the semiconductor. The first observation of higher excited excitons, called Rydberg excitons, first in a cuprous oxide bulk [16] and then in nanostructures [19] revealed a lot of their astonishing features, such as an extraordinarily large dimension scaling as n^2, long life-times $\sim n^3$, reaching nanoseconds. Their extraordinary vulnerability to interactions with external fields is due to huge polarizability scaling as n^7.

Another characteristic property of excitons is the so-called Rydberg blockade. For a given exciton with principal quantum number n, another exciton cannot be created in the immediate vicinity due to the exciton-exciton interaction that shifts the energy levels. The space where another exciton cannot be created is described by a so-called blockade volume [16]

$$V_B = 3 \times \ 10^{-7} n^7 \ \mu\mathrm{m}^3. \tag{1}$$

The crucial feature is the extremely fast n^7 scaling of the blockade; highly excited states very quickly reach the saturation level when the medium is completely filled with excitons. As a result, the light propagating through the medium is not absorbed to create new excitons. This is the so-called optical bleaching. On the other hand, the lowest excitonic states can reach a considerable density. Specifically, for $n = 2$, taking into account a semi-random distribution of blockade volumes as opposed to ideal sphere packing [23] one obtains an upper density limit on the order of 10^{17} cm^{-3}, with some sources reporting even 10^{19} cm^{-3} densities [24]. The issue of maximum possible density is important to the effect of excitonic transitions on surface plasmons; specifically, the propagation properties of SPP are dependent on the Cu_2O permittivity $\epsilon = 7.5 + \chi$, where the changes of susceptibility χ caused by excitons are directly proportional to exciton density. It is beneficial to obtain conditions where these susceptibility changes are not negligible when compared with the "static" part $\epsilon_b = 7.5$. This can be only achieved with the lowest excitonic states. Furthermore, another reason to consider only the lowest P-excitonic states ($n = 2, 3$) is the interaction of excitons with metallic surfaces. As mentioned above, excitons with a high principal quantum number are very sensitive to external electric fields, including electrostatic fields at the metal-dielectric interface [25], leading to ionization of excitons that are separated from the metal surface by a distance comparable to the exciton radius. Thus, for example, one can expect that the $n = 2$ exciton in Cu_2O is strongly affected by the metallic environment when located closer than approximately 6 nm from the metal-dielectric interface.

III. PROPAGATION OF SURFACE PLASMONS

Surface plasmon is a localized electromagnetic excitation on an interface between two media with exhibit opposite signs of dielectric permittivity at some frequency ω. Typically, the material with negative permittivity $\epsilon_1(\omega)$ is a metal and the other one characterized by $\epsilon_2(\omega) > 0$ is a dielectric. In such a system, with the help of Maxwell's equations, one can derive the wave vector of a electromagnetic wave mode that propagates along the metal-dielectric interface [26]

$$\kappa(\omega) = \kappa' + i\kappa'' = \frac{\omega}{c}\sqrt{\frac{\epsilon_1\epsilon_2}{\epsilon_1 + \epsilon_2}}, \tag{2}$$

where κ' and κ'' are the real and imaginary parts of the wave vector component, respectively, and c is the speed of light in a vacuum. For real values of ϵ_1 and ϵ_2, one obtains the real wave vector when $\epsilon_1\epsilon_2 < 0$ and $\epsilon_1 + \epsilon_2 < 0$ and in such a case propagating SPPs can be excited.

In this paper, we will consider a metal layer of finite thickness d. In such a case, one obtains modified boundary conditions which result in two solutions [27,28]

$$\begin{aligned} \frac{\kappa_1 \tanh\left(\kappa_1 \frac{d}{2}\right)}{\epsilon_1} &= \frac{-\kappa_2}{\epsilon_2}, \\ \frac{\kappa_1 \coth\left(\kappa_1 \frac{d}{2}\right)}{\epsilon_1} &= \frac{-\kappa_2}{\epsilon_2}, \end{aligned} \tag{3}$$

where $\kappa_{1,2} = \sqrt{k^2 - \epsilon_{1,2}\frac{\omega^2}{c^2}}$. In the limit of $d \to \infty$, Eqs. (3) reduce to the form given by Eq. (2). The two above solutions are the so-called short-range and long-range plasmons (SRSPP, LRSPP, accordingly). They are characterized by a small or large group velocity

$$V_g = \frac{\partial\omega}{\partial\kappa'} = \frac{c}{n_{\mathrm{eff}} + \omega\frac{\partial n_{\mathrm{eff}}}{\partial\omega}}, \tag{4}$$

where $n_{\mathrm{eff}} = \sqrt{\epsilon}$ is the effective refraction index. The crucial property of long-range plasmons is reduced absorption and elevated group velocity, which allows them to propagate over distances on the order of tens to hundreds of μm [29–32]. One can take an advantage of this to produce relatively long-living plasmons in copper. As mentioned before, in some cases the ohmic losses in Cu-based systems can approach the values typical to silver and gold nanostructures, provided that the detrimental effects of the oxide layer are mitigated. Here, we propose a system where the Cu_2O is an inherent part of the structure necessary for its operation. Particularly, we consider a thin layer of Cu surrounded by semi-infinite (much thicker than wavelength) layers of Cu_2O. The system is shown on the Fig. 1(a). An external light source (point source of radiation in the FDTD calculations, described in Appendix) generates both long- and short-range excitons; they can be seen on the Fig. 1(b), where the field distribution is symmetric or antisymmetric for LRSPP and SRSPP, accordingly.

To derive the optical properties of the proposed system, one needs a suitable model of the materials. In the considered spectral range of 2–2.2 eV, the permittivity of the oxide is very close to a constant $\epsilon_2 = 7.5$, with the additional impact of excitons as outlined in the next section. For the properties of copper, we refer to [33]. The real and imaginary parts of permittivity and the fitted model used in FDTD calculations are shown on the Fig. 2. The model is fitted to provide a good match in the spectral region of Rydberg excitons, marked by dashed lines; specifically, the maximum difference between experimentally measured susceptibility and the model is less than 2% in a 100-meV range around the $2P$ exciton energy, which is considerably more than the spectral width of simulated plasmons. Two main features of the susceptibility

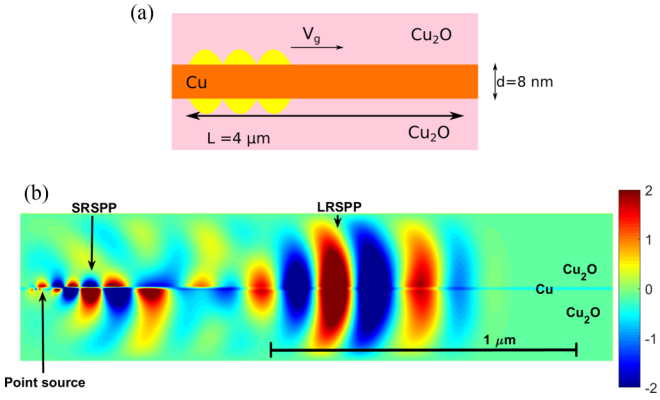

FIG. 1. (a) Schematic representation of the system considered in the paper. Surface plasmon (yellow) propagates along the metal surface at some group velocity V_g. (b) Spatial distribution of normalized electric field (color) obtained in FDTD simulation.

relation $\epsilon_1(\omega)$ are apparent; there is a considerable increase of absorption (proportional to the imaginary part of permittivity), which is the result of interband transitions in Cu [33]. This increase starts just above the gap energy of Cu_2O, so that the excitons, which have energies smaller than the band gap, still remain in the low absorption part of the spectrum. Furthermore, the real part of permittivity is negative, and in fact, in the spectral region of excitons, it provides a close match to the oxide permittivity, e.g., $\epsilon_1 + \epsilon_2 \approx 0$. This is a crucial condition for excitation of strong plasmonic resonance; these findings are consistent with [34], where a strong plasmonic resonance in the region of 2 eV was demonstrated in a thin copper film.

IV. TUNABLE LONG-RANGE PLASMONS

Let's consider a long-range plasmon propagating along a thin layer of Cu surrounded by Cu_2O. By using the above-discussed model of metal permittivity ϵ_1 and the oxide permittivity ϵ_2 containing a numerically calculated excitonic

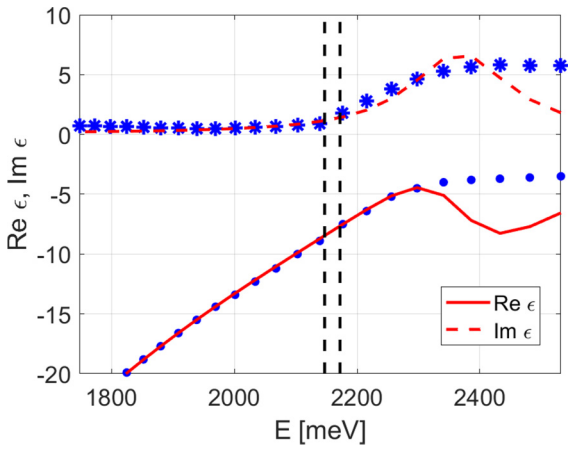

FIG. 2. Copper permittivity data from [33] (dots) and the fitted model (lines). Dashed black lines mark the part of the spectrum occupied by Rydberg excitons in Cu_2O, indicating energy of $2P$ exciton and gap energy.

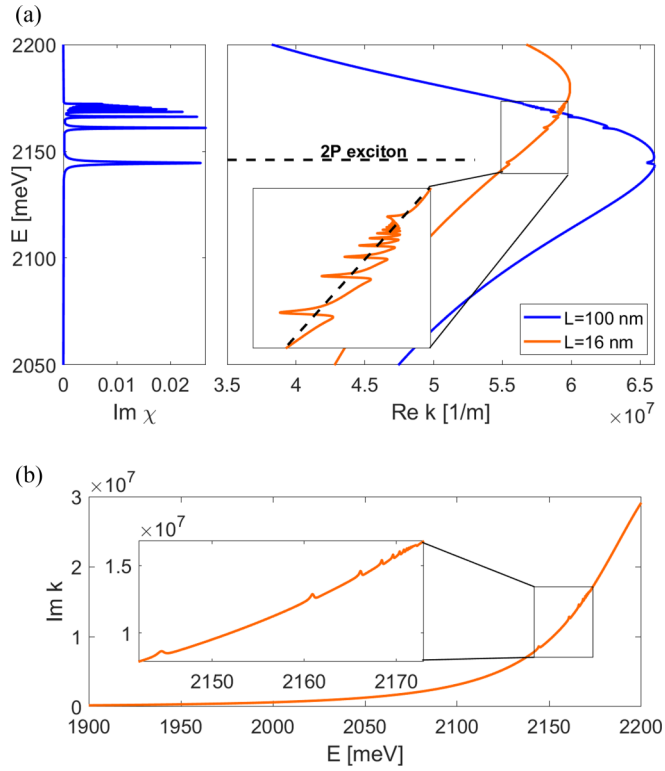

FIG. 3. (a) Dispersion relation of surface plasmon calculated for a case of thick and thin layers of Cu. Inset: Part of the relation containing excitonic resonances. Dashed line marks the dispersion relation without exciton contribution. (b) Imaginary part of wave vector k as a function of energy.

spectrum [35], we can calculate the exciton wave vector from Eq. (3). The results are shown in Fig. 3(a). The left panel shows the Cu_2O susceptibility $\chi(\omega) = \epsilon_2(\omega) - 7.5$ exhibiting the characteristic spectrum of Rydberg excitons with multiple states corresponding to principal quantum number $n = 1, 2, \ldots, 20$. These resonances have a noticeable impact on the dispersion curve $\kappa(\omega)$ (right panel, inset). While the absolute value of the changes of ϵ_2 caused by excitons is rather small, these changes occur in a very narrow spectral range of excitonic resonances. This means that the group velocity of plasmon, which is connected with the slope of the function $\kappa(\omega)$ according to Eq. (4), is significantly affected by the excitons. This is a key component of our proposal of tunable plasmons. Due to the change of the plasmon group velocity, the time needed to propagate some certain distance is changed. This, in turn, affects the amount of plasmon energy absorbed by the metal due to the ohmic losses. As a result, we can significantly change the transmission coefficient of the system despite the fact that direct absorption by Cu_2O is negligible when compared to Cu. In Fig. 3(b) one can see the imaginary part of the plasmon wave vector, which is responsible for absorption. The steady increase of absorption with energy is directly linked to the copper susceptibility; the local maxima of absorption caused by excitons (inset) is a secondary effect. Another crucial component of our proposal is the use of a thin Cu layer. One can see that the dispersion relation in Fig. 3(a) calculated for a thick layer changes from

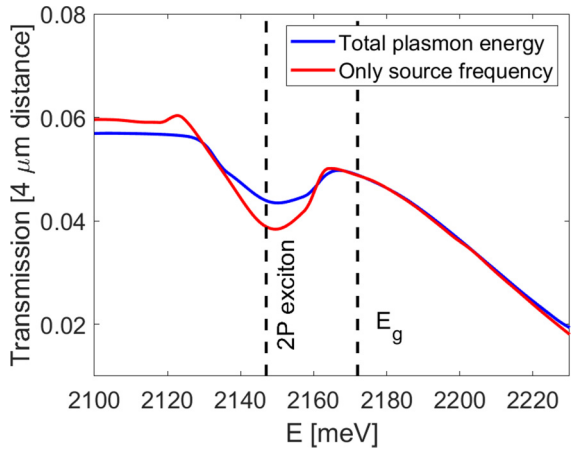

FIG. 4. Transmission coefficient of long-range plasmons on a thin Cu layer.

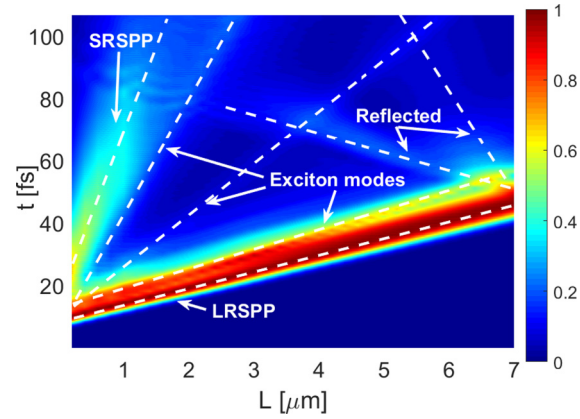

FIG. 5. Normalized field amplitude (color) of excited plasmonic modes as a function of time and position along the metal layer.

a normal dispersion below 2.14 eV to anomalous dispersion above (e.g., the value of κ is decreasing with energy). However, by using a sufficiently thin layer, one can increase the energy where the transition to anomalous dispersion occurs; the same technique was used in [36] to facilitate the propagation of UV plasmons. In the case here, it allows for the excitation of plasmons in the 2.1–2.2 eV range, fitted to the spectral region of Rydberg excitons. Specifically, Fig. 3 inset shows the dispersion relation of such plasmons. One can see that the general slope of the function $\omega(\kappa)$ is steeper than in the thick layer case, indicating an increased group velocity of LRSPPs. At the same time, the slope of $\omega(\kappa)$ near excitonic resonances is considerably smaller, corresponding to a greatly reduced group velocity. As discussed in [37], group velocities on the order of 10^3 m/s are possible for a light pulse tuned to $n > 10$ exciton propagating in Cu_2O. In the case of the low n excitonic states and plasmons considered here, the slowdown is less considerable since the plasmon dispersion relation depends on the permittivity of both dielectric and metal, the effect of the excitonic resonances is reduced. Furthermore, the spectrum of the plasmon is much wider than the width of excitonic resonance, so that only selected spectral components of SPP are affected by the exciton. This is discussed further below. Finally, from a practical point of view, apart from the potential irregularity of the oxidation film (Cu_2O), the close separation of higher excitonic resonances prevents them from being selectively excited by a relatively short-living, wide spectrum plasmon.

The FDTD results, where the transmission coefficient T of LRSPP propagates through a distance of $L = 4$ μm on a $d = 8$-nm-thick Cu layer is calculated, is shown in Fig. 4. Notably, transmission coefficient on the order of 5% is obtained, which is considerably bigger than can be achieved with bulk plasmons, even with noble metals [32]. The two transmission coefficients shown in Fig. 4 correspond to the entire plasmon and its central frequency. Specifically, the total transmission (blue) is calculated directly from the field amplitude obtained in FDTD simulation, while the central/source frequency transmission is obtained by applying a narrow band pass filter to the numerical data. One can see a noticeable drop of transmission in the region of the strongest $2P$ exciton. This minimum is more pronounced when only the central frequency is considered. This is caused by the fact that the spectrum of the propagating plasmon is considerably wider that the excitonic resonance. Specifically, in this particular case the plasmon lifetime is on the order of 10^{-13} s, corresponding to the spectral width $\Delta E \sim 30$ meV. This value is comparable to the distance between $n = 2$ and $n = 3$ excitonic states (14 meV) and approximately six times larger than the widest resonance of the $n = 2$ exciton (5 meV) [16]. Correspondingly, the exciton lifetime is several times longer than the plasmonic lifetime, being equal to $\tau \sim 1$ ps for $n = 2$. Finally, while the low-n excitons are considerably smaller than the space occupied by the propagating plasmon ($2P$ exciton radius is approximately $r_E = 1.5$ nm, blockade radius $r_B = 19$ nm), they can easily exceed the plasmon size for larger n. This particular set of size and lifetime proportions has several important consequences.

(1) The local reduction of the group velocity is applied only to some wave modes close to the central frequency of excitonic resonance and not the entire plasmon spectrum. This means that the effectiveness of the slowdown of a surface plasmon as a whole is reduced and, in general, a single group velocity cannot be attributed to the plasmon (e.g., there is considerable group velocity dispersion).

(2) By fine-tuning the frequency of the light exciting the plasmon, one can effectively aim at $n = 2$ and $n = 3$ excitonic states; higher states are located too closely to each other to be targeted selectively in such a system. However, this restriction does not apply when a second, nonplasmon field is used to excite some specific state, which is then used in the exciton-plasmon interaction.

(3) The locally enhanced absorption of specific modes produces a narrow dip in the plasmon spectrum, similar to the so-called spectral hole-burning [38].

To confirm the above findings and further investigate the plasmon dynamics and its interaction with excitons, one can analyze the group velocity of excited plasmonic modes by considering the electric field amplitude as a function of time and position, as shown in Fig. 5. The figure is dominated by two strong lines representing LRSPP and SRSPP modes;

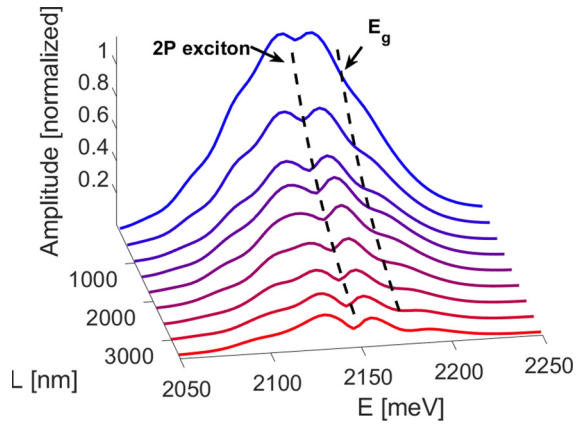

FIG. 6. Frequency spectra of the propagating LRSPP calculated at various propagation lengths.

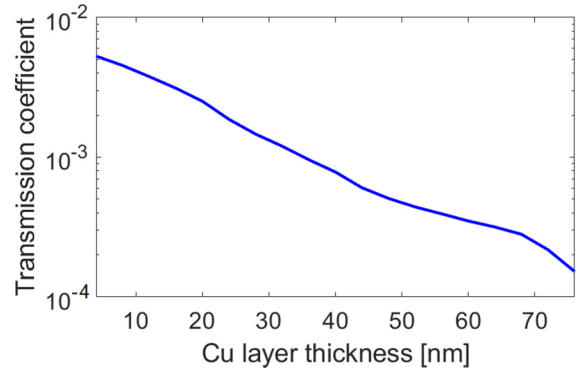

FIG. 7. Transmission coefficient over the distance $L = 4\ \mu$m as a function of metal layer thickness d.

their slope differs considerably, indicating group velocities on the order of 0.3 c and 0.04 c, accordingly. One can also see that the long-range plasmon maintains nonnegligible amplitude after reaching the end of the computation domain at $L = 4\ \mu$m, and then it is reflected. At the point of reflection, both long-range and short-range modes are created (more horizontal and vertical lines, accordingly). Finally, one can notice weaker traces of several modes with group velocities that differ considerably from the LRSPP. These modes correspond to the spectral range of the $2P$ exciton, specifically in the regions of increased normal dispersion around the excitonic resonance. As mentioned before, due to the reduction of group velocity, these modes are more strongly absorbed by the metal. Moreover, since the group velocity change caused by excitonic resonance occurs in a very narrow part of the spectrum, being only a fraction of the plasmon spectrum, the slow modes carry relatively little energy and thus are barely visible in Fig. 5. A somewhat explicit picture can be obtained by considering the image of the plasmon in the frequency domain. The spectrum of LRSPP is shown in Fig. 6. One can see how the plasmon spectrum evolves with the propagation length; initially, it is approximately a Gaussian with the width on the order of 100 meV. However, as the plasmon propagates along the metal surface, a noticeable dip is formed at the energy of 2147 meV, which corresponds to the $2P$ exciton resonance. Another, weaker local minimum is present above the band-gap energy $E_g = 2172$ meV. This means that the increased absorption of Cu_2O in the region above the band gap is a relatively minor contribution to absorption as compared to the slowdown of V_g and subsequent absorption by Cu. After the propagation distance of $L = 3\ \mu$m, the local minimum in the spectrum is quite substantial, with approximately 30% lower amplitude. This is consistent with the results in Fig. 4, where a local reduction of the transmission coefficient from 6% to 4% is shown. It should be stressed that the LRSPP is not an ideal Gaussian but a collection of modes that propagate at various group velocities that can differ considerably; this complicates the calculation of the spectrum and is the cause of other local minima visible in Fig. 6. However, in contrast to the minimum corresponding to the $2P$ exciton, these apparent minima do not appear consistently in each spectrum, at the same energy. Finally, from Fig. 1(b) one can see that the electric field of plasmons extends into Cu_2O up to a distance of $\sim$300 nm from the metal surface; therefore, the plasmon field can easily reach excitons that are not strongly affected by the immediate vicinity of the metal-oxide interface and the use of unperturbed energy of the $2P$ exciton state $E_{2P} = 2147$ meV in calculations is justified.

As mentioned before, the strength of the optical response of Cu_2O is directly proportional to the exciton density. This, in turn, depends on the energy provided to generate the excitons and is limited by the Rydberg blockade. As a result, one has several options for dynamically controlling the system.

(1) When the propagating plasmon's frequency is tuned to the excitonic resonance, its energy can be used to create new excitons. In such a case, the response of the system (transmission coefficient) will be highly dependent on the power of the plasmon.

(2) One can use the external optical field (control field) to create a given density of excitons, which then affects the propagation of weaker probe field (plasmon).

(3) Due to the narrow spectrum of excitonic resonances, only a slight detuning of the plasmon frequency is needed to considerably affect its transmission.

(4) By exciting two plasmons in a short period, one can potentially create conditions where the excitons generated by the first plasmon affect the propagation of the second plasmon, allowing for exciton-mediated plasmon-plasmon interactions.

(5) In a similar manner, one can arrange the interaction between plasmons propagating along two closely spaced metal layers.

From the point of view of practical applications, it is important to consider the maximum thickness of the Cu layer that allows for the propagation of long-range plasmons. As mentioned in [32], the thickness d should be considerably smaller than the plasmon wavelength. In Fig. 1(b), one can estimate that this wavelength is about 200 nm (the vacuum wavelength of incident light is $\lambda = 577$ nm, which indicates that the effective refraction index is $n_{\text{eff}} \approx 2.9$; this is slightly larger than the index of Cu_2O $n_2 = 2.73$). Therefore, one can assume that the metal layer thickness must be $d \ll 200$ nm. This is the case in Fig. 7; the transmission coefficient decreases exponentially with the layer thickness, with a value of $T \sim 4\%$ for $d = 10$ nm and $T \sim 0.1\%$ for $d = 35$ nm.

V. CONCLUSION

The discovery of Rydberg excitons in Cu_2O has opened many new perspectives in semiconductor science, but also posed many theoretical problems and challenges. While the optical properties of REs, especially in bulk media, are already well understood, the ongoing research on Rydberg excitons is now entering the phase where the first experiments involving confined systems are performed. Thus, it is of high importance to provide the theoretical framework for understanding the properties of these highly complex media. Metallic nanostructures and the exciton-plasmon interaction are one of the promising directions of study. Due to the inherent losses in Cu, regular plasmon modes alone are not suitable as carriers of information over the long distances. However, as we demonstrated, the so-called long-range plasmons can achieve propagation length on the order of micrometres. At this scale, it is possible to couple them with excitons in Cu_2O, allowing for many interesting options to dynamically control the plasmon propagation. It is shown that the group velocity of the propagating plasmon can be significantly affected by the presence of excitons, which affects the system transmission. The presented results may pave the way to compact, copper-based tunable devices.

APPENDIX: FDTD METHOD

One of the most popular tools for the numerical analysis of SPP propagation is the finite-difference time-domain (FDTD) method [39]. It is based directly on Maxwell's equations, which provides a high flexibility and accuracy in modeling the propagation of electromagnetic waves. In this paper, we focus on the two-dimensional variant of the method; the computational domain is a cross-section of the system placed on the xy plane. The structure is assumed to be symmetric and semi-infinite (e.g., much larger than light wavelength) in the z direction. The domain is divided into a rectangular grid of discrete cells with the size $\Delta x = 4$ nm. In every cell, the values of the components of the fields $\vec{E}(x, y, t)$, $\vec{H}(x, y, t)$ are stored. By defining a discrete time step Δt, one can use the Maxwell's equations to derive the evolution equations that use the field values $\vec{E}(x, y, t)$, $\vec{H}(x, y, t)$ to calculate the next ones $\vec{E}(x, y, t + \Delta t)$, $\vec{H}(x, y, t + \Delta t)$. In the two-dimensional case, without loss of generality one can assume that the fields have only three nonzero components $\vec{E} = [E_x, E_y, 0]$, $\vec{H} = [0, 0, H_z]$. The optical response of materials in the simulation is described by the polarization vector $\vec{P}(x, y, t)$. Specifically, one can use the so-called Drude-Lorentz model that specifies the connection between the electric field in polarization in the frequency domain

$$\begin{aligned} \vec{P}(\omega) &= \epsilon(\omega)\vec{E}(\omega), \\ \epsilon(\omega) &= \epsilon_\infty + \sum_{j=1}^{n} \frac{\omega_{pj}^2}{\omega_{0j}^2 - \omega^2 - i\gamma_j\omega}, \end{aligned} \tag{A1}$$

with a set of n oscillators with the so-called plasma frequency ω_{pj}, resonance frequency ω_{0j}, and dissipation constant γ_j. In the case of Cu, one can use two oscillators; the first one with $\omega_{p1} = 0$ describes the baseline Drude model of free electrons in metal, while the second oscillator provides the correction responsible for the increase of absorption due to the interband transitions (the local maximum at $E = 2370$ meV in Fig. 2). For Cu_2O, one has $\epsilon_\infty = 7.5$ and the series of oscillators corresponding to excitonic resonances, with appropriate oscillator strengths and damping constants. The medium model was verified by comparing the numerically obtained absorption spectrum of Cu_2O with the results in [16]. In the performed calculations, the plasmon center frequency is tuned to the $n = 2$ exciton and thus an inclusion of two excitons $n = 2$ and $n = 3$ provides sufficient accuracy of results. The above medium frequency response is integrated into time domain simulation with the use of the axillary differential equations (ADE) approach [40]. In this method, one can calculate the polarization as a function of time with the following differential equation:

$$\ddot{P} + \gamma_j\dot{P} + \omega_{0j}^2 P = \frac{\omega_{pj}^2}{\epsilon_\infty} E \tag{A2}$$

for every oscillator j. The final set of equations based on Eq. (A2) and Maxwell's equation is as follows:

$$\begin{aligned} \frac{\partial E_y(x, y, t)}{\partial x} - \frac{\partial E_x(x, y, t)}{\partial y} &= -\mu_0 \frac{\partial H_z(x, y, t)}{\partial t}, \\ \frac{\partial H_z(x, y, t)}{\partial y} &= j_x(x, y, t) + \epsilon_0 \frac{\partial E_x(x, y, t)}{\partial t} \\ &\quad - \frac{\partial P_x(x, y, t)}{\partial t}, \\ -\frac{\partial H_z(x, y, t)}{\partial x} &= j_y(x, y, t) + \epsilon_0 \frac{\partial E_y(x, y, t)}{\partial t} \\ &\quad + \frac{\partial P_y(x, y, t)}{\partial t}, \end{aligned} \tag{A3}$$

where the polarization has two components P_x, P_y which depend on E_x, E_y according to Eq. (A2). The j_x and j_y are the current densities in the corresponding directions and ϵ_0, μ_0 are vacuum permittivity and permeability. By rearranging the terms in Eq. (A3), one can express the future values of the fields $E_x(x, y, t + 1)$, $E_y(x, y, t + 1)$, $H_z(x, y, t + 1)$ as a function of the current values. Such relations allow for advancing the state of the system in discrete time steps by calculating the new field values based on the current ones.

The frequency scaling of the simulation is set so that a single spatial step $\Delta x = 4$ nm. The material parameters are given in Table I below. Copper is modeled with the Drude model (e.g., free electrons with no intrinsic resonance frequency $\omega_{01} = 0$) with an additional oscillator to include the interband transitions. In the copper oxide, only the strongest $2P$ exciton is modeled.

TABLE I. Model parameters for materials used in FDTD simulation.

Material	ϵ_∞	ω_{01}	ω_1	γ_1	ω_{02}	ω_2	γ_2
Cu	15.3	0	0.2236	0.00005	0.048	0.0361	0.004
Cu_2O	7.5	0.0433	0.0000007	0.0001	0	0	0

[1] A. Böhme, F. Sterl, E. Kath, M. Ubl, V. Manninen, and H. Giessen, Electrochemistry on inverse copper nanoantennas: Active plasmonic devices with extraordinarily large resonance shift, ACS Photonics **6**, 1863 (2019).

[2] C. de Melo, M. Jullien, Y. Battie, A. Naciri, J. Ghanbaja, F. Montaigne, J. Pierson, F. Rigoni, N. Almqvist, A. Vomiero, S. Migot, F. Mücklich, and D. Horwat, Tunable localized surface plasmon resonance and broadband visible photoresponse of Cu nanoparticles/ZnO surfaces, ACS Appl. Mater. Interfaces **10**, 40958 (2018).

[3] C. Huang, G. Kumar, G. Sharma, and F. Chen, Plasmonic effects of copper nanoparticles in polymer photovoltaic devices for outdoor and indoor applications, Appl. Phys. Lett. **116**, 253302 (2020).

[4] D. Fedyanin, D. Yakubovsky, R. Kirtaev, and V. Volkov, Ultralow-loss CMOS copper plasmonic waveguides, Nano Lett. **16**, 362 (2016).

[5] V. G. Kravets, R. Jalil, Y. J. Kim, D. Ansell, D. E. Aznakayeva, B. Thackray, L. Britnell, B. D. Belle, F. Withers, I. P. Radko, Z. Han, S. I. Bozhevolnyi, K. S. Novoselov, A. K. Geim, and A. N. Grigorenko, Graphene-protected copper and silver plasmonics, Sci. Rep. **4**, 5517 (2014).

[6] G. Chan, J. Zhao, E. Hicks, G. Schatz, and R. Van Duyne, Plasmonic properties of copper nanoparticles fabricated by nanosphere lithography, Nano Lett. **7**, 1947 (2007).

[7] O. Peña-Rodríguez and U. Pal, Effects of surface oxidation on the linear optical properties of Cu nanoparticles, J. Opt. Soc. Am. B **28**, 2735 (2011).

[8] J. Sancho-Parramon, B. Okorn, K. Salamon, and V. Janicki, Plasmonic resonances in copper island films, Appl. Surf. Sci. **463**, 847 (2019).

[9] V. Mkhitaryan, K. March, E. Tseng, X. Li, L. Scarabelli, L. Liz-Marzán, S. Chen, L. Tizei, O. Stéphan, J. Song, M. Kociak, F. Garcia, and A. Gloter, Can copper nanostructures sustain high-quality plasmons?, Nano Lett. **21**, 2444 (2021).

[10] N. Fofang, T. Park, O. Neumann, N. Mirin, P. Nordlander, and N. Halas, Plexcitonic nanoparticles: Plasmon-exciton coupling in nanoshell-J-aggregate complexes, Nano Lett. **8**, 3481 (2008).

[11] E. Karademir, S. Balci, C. Kocabas, and A. Aydinli, Plexcitonic crystals: A tunable platform for light-matter interactions, Opt. Express **22**, 21912 (2014).

[12] H. Lee, D. Luong, M. Kim, Y. Jin, H. Kim, S. Yun, and Y. Lee, Reconfigurable exciton-plasmon interconversion for nanophotonic circuits, Nat. Commun. **7**, 13663 (2016).

[13] E. Cao, W. Lin, M. Sun, W. Liang, and Y. Song, Exciton-plasmon coupling interactions: From principle to applications, Nanophotonics **7**, 145 (2018).

[14] P. A. D. Gonçalves, L. Bertelsen, S. Xiao, and N. Mortensen, Plasmon-exciton polaritons in two-dimensional semiconductor/metal interfaces, Phys. Rev. B **97**, 041402(R) (2018).

[15] J. Khurgin, Pliable polaritons: Wannier exciton-plasmon coupling in metal-semiconductor structures, Nanophotonics **8**, 629 (2019).

[16] T. Kazimierczuk, D. Fröhlich, S. Scheel, H. Stolz, and M. Bayer, Giant Rydberg excitons in the copper oxide Cu_2O, Nature (London) **514**, 343 (2014).

[17] A. Poddubny and M. Glazov, Topological Spin Phases of Trapped Rydberg Excitons in $Cu2_O$, Phys. Rev. Lett. **123**, 126801 (2019).

[18] D. Ziemkiewicz, G. Czajkowski, K. Karpiński, and S. Zielińska-Raczyńska, Rydberg magnetoexcitons in Cu_2O quantum wells, Phys. Rev. B **103**, 035305 (2021).

[19] K. Orfanakis, S. Rajendran, H. Ohadi, S. Zielińska-Raczyńska, G. Czajkowski, K. Karpiński, and D. Ziemkiewicz, Quantum confined Rydberg excitons in Cu_2O nanoparticles, Phys. Rev. B **103**, 245426 (2021).

[20] A. Konzelmann, B. Frank, and H. Giessen, Quantum confined Rydberg excitons in reduced dimensions, J. Phys. B: At. Mol. Opt. Phys. **53**, 024001 (2020).

[21] S. Steinhauer, M. Versteegh, S. Gyger, A. Elshaari, B. Kunert, A. Mysyrowicz, and V. Zwiller, Rydberg excitons in Cu2O microcrystals grown on a silicon platform, Commun. Mater. **1**, 2 (2020).

[22] M. Takahata, K. Tanaka, and N. Naka, Nonlocal optical response of weakly confined excitons in Cu_2O mesoscopic films, Phys. Rev. B **97**, 205305 (2018).

[23] C. Morin, J. Tignon, J. Mangeney, S. Dhillon, G. Czajkowski, K. Karpiński, S. Zielińska-Raczyńska, D. Ziemkiewicz, and T. Boulier, Self-Kerr Effect across the Yellow Rydberg Series of Excitons in Cu_2O, Phys. Rev. Lett. **129**, 137401 (2022).

[24] G. M. Kavoulakis, G. Baym, and J. P. Wolfe, Quantum saturation and condensation of excitons in Cu_2O: A theoretical study, Phys. Rev. B **53**, 7227 (1996).

[25] M. Kohlhoff, Interaction of Rydberg atoms with surfaces, Eur. Phys. J.: Spec. Top. **225**, 3061 (2016).

[26] E. Chubchev, I. Nechepurenko, A. Dorofeenko, A. Vinogradov, and A. Lisyansky, Highly confined surface plasmon polaritons in the ultraviolet region, Opt. Express **26**, 9050 (2018).

[27] H. Raether, *Surface plasmons on smooth surfaces*, in Surface Plasmons on Smooth and Rough Surfaces and on Gratings (Springer, New York, 1988), pp. 4–39.

[28] D. Ziemkiewicz, K. Słowik, and S. Zielińska-Raczyńska, Ultraslow long-living plasmons with electromagnetically induced transparency, Opt. Lett. **43**, 490 (2018).

[29] V. Konopsky, E. Alieva, Long-Range Propagation of Plasmon Polaritons in a Thin Metal Film on a One-Dimensional Photonic Crystal Surface, Phys. Rev. Lett. **97**, 253904 (2006).

[30] R. Yi, L. Fang, H. Yi-Dong, D. Ohnishi, Z. Wei, and P. Jiang-De, Long-range surface plasmon polaritons guided by a thin metal stripe, Chin. Phys. Lett. **24**, 1626 (2007).

[31] S. Park, J. Jin Ju, J. Tae Kim, M. Kim, S. Koo Park, J. Lee, W. Lee, and M. Lee, Sub-dB/cm propagation loss in silver stripe waveguides, Opt. Express **17**, 697 (2009).

[32] P. Berini, Long-range surface plasmon polaritons, Adv. Opt. Photon. **1**, 484 (2009).

[33] T. Hollstein, U. Kreibic, and F. Lens, Optical properties of Cu and Ag, Phys. Stat. Sol. (b) **82**, 545 (1977).

[34] K. Takagi, S. Nair, R. Watanabe, K. Seto, T. Kobayashi, and E. Tokunaga, Surface plasmon polariton resonance of gold, silver, and copper studied in the kretschmann geometry: Dependence on wavelength, angle of incidence, and film thickness, J. Phys. Soc. Jpn. **86**, 124721 (2017).

[35] S. Zielińska-Raczyńska, G. Czajkowski, and D. Ziemkiewicz, Optical properties of Rydberg excitons and polaritons, Phys. Rev. B **93**, 075206 (2016).

[36] K. Karpiński, S. Zielińska-Raczyńska, and D. Ziemkiewicz, Long-range plasmons and epsilon-near-zero modes in ultraviolet, J. Opt. Soc. Am. B **38**, 79 (2021).

[37] H. Stolz, F. Schöne, and D. Semkat, Interaction of Rydberg excitons in cuprous oxide with phonons and photons: Optical linewidth and polariton effect, New J. Phys. **20**, 023019 (2018).

[38] U. Wahid, A. Khan, B. Amin, and A. Ullah, Surface plasmon hole burning at the interface of Cesium and Gold by Kerr nonlinearity, Optik **202**, 163651 (2020).

[39] K. S. Yee, Numerical solution of initial boundary value problems involving Maxwell's equations in isotropic media, IEEE Trans. Antennas Propag. **14**, 302 (1966).

[40] M. A. Alsunaidi and A. Al-Jabr, A general ADE-FDTD algorithm for the simulation of dispersive structures, IEEE Photon. Techol. Lett. **21**, 817 (2009).